

In Search of ... η Car

Rubab Khan, K. Z. Stanek, and C. S. Kochanek (The Ohio State University)

Abstract: We utilize *Spitzer* IRAC images of 7 nearby galaxies to search for possible analogs of η Carinae. We select 34 objects as candidates that have a flat or rising mid-IR spectral energy distribution, emit $>10^5 L_{\odot}$ in the IRAC bands (3.6 to 8.0 μm), and are not known to be a background source. Based on our estimates for the expected number of background sources in our data, we expect that follow-up observations will show that many of these candidates are either non-stellar or are not truly analogous to η Car. Having only 34 candidates already indicates that Great Eruptions are rare and their frequency, at most, is comparable to the ccSN rate.

Why are they interesting?

Understanding the evolution of massive stars such as luminous blue variable, red super giants and Wolf-Rayet stars is challenging even when mass loss is restricted to continuous winds. But poorly understood impulsive mass ejections may well be the dominant mass loss mechanism (Humphreys & Davidson 1984, Kochanek 2011). At the high mass-loss rates of eruptions, dust forms and the star will be heavily obscured for an extended period after an eruption, as η Carinae is now, 160 years after the Great Eruption (Figure 1). This means that dusty ejecta are a powerful and long-lived signature of eruption. The emission from these dusty envelopes peaks in the mid-IR, with a characteristic red color and a rising or flat spectral energy distribution (SED, λL_{λ}) in the *Spitzer* IRAC bands (Figure 2). Quantifying the rarity of η Car analogs in the local universe allows us to investigate the rate of giant eruptions of the most massive stars.

How Do We Search for Them?

We selected 7 galaxies spanning a range of mass, morphology, distance, and star formation history: NGC6822, M33, NGC300, M81, NGC2403, NGC247 and NGC7793. After building up a catalog of sources that emit $\nu L_{\nu} > 10^4 L_{\odot}$ in at least one of the three shorter (3.6, 4.5, 5.8 μm) IRAC bands, we determine the integrated mid-IR luminosity ($L_{\text{mid-IR}}$), the slope (a , $\lambda L_{\lambda} \propto \lambda^a$) of the mid-IR SEDs, and the fraction (f) of $L_{\text{mid-IR}}$ that is emitted in the three shorter bands for each source. We initially select objects with $L_{\text{mid-IR}} > 10^5 L_{\odot}$, $a > 0$ and $f > 0.3$, and reject a source as non-stellar if it is a galaxy or AGN with a measured redshift or if archival images show that it is unambiguously a galaxy (Figure 3, left panel). We measure the far-IR luminosity from the *Spitzer* MIPS images, although the 60 and 170 μm results are only upper limits.

What Do We Find?

We initially detect 46 sources that met our selection criteria and reject 11 of these as non-stellar background sources. We re-discovered "Object X", the brightest mid-IR star in M33 and the subject of Khan et. al. (2011). The other 34 sources remain as candidates. Based on our estimate of the expected extragalactic contamination (Figure 3, right panel) using the SDWFS survey (Ashby et. al. 2009), we expect a total of ~ 41 extragalactic sources to pass the selection criteria. Moreover, even a casual look at the SEDs of the 34 candidate sources show that only a handful of them have SEDs that closely resemble the SED of η Carinae (Figures 4 and 5). So, very few of the remaining candidates can be actual stellar sources.

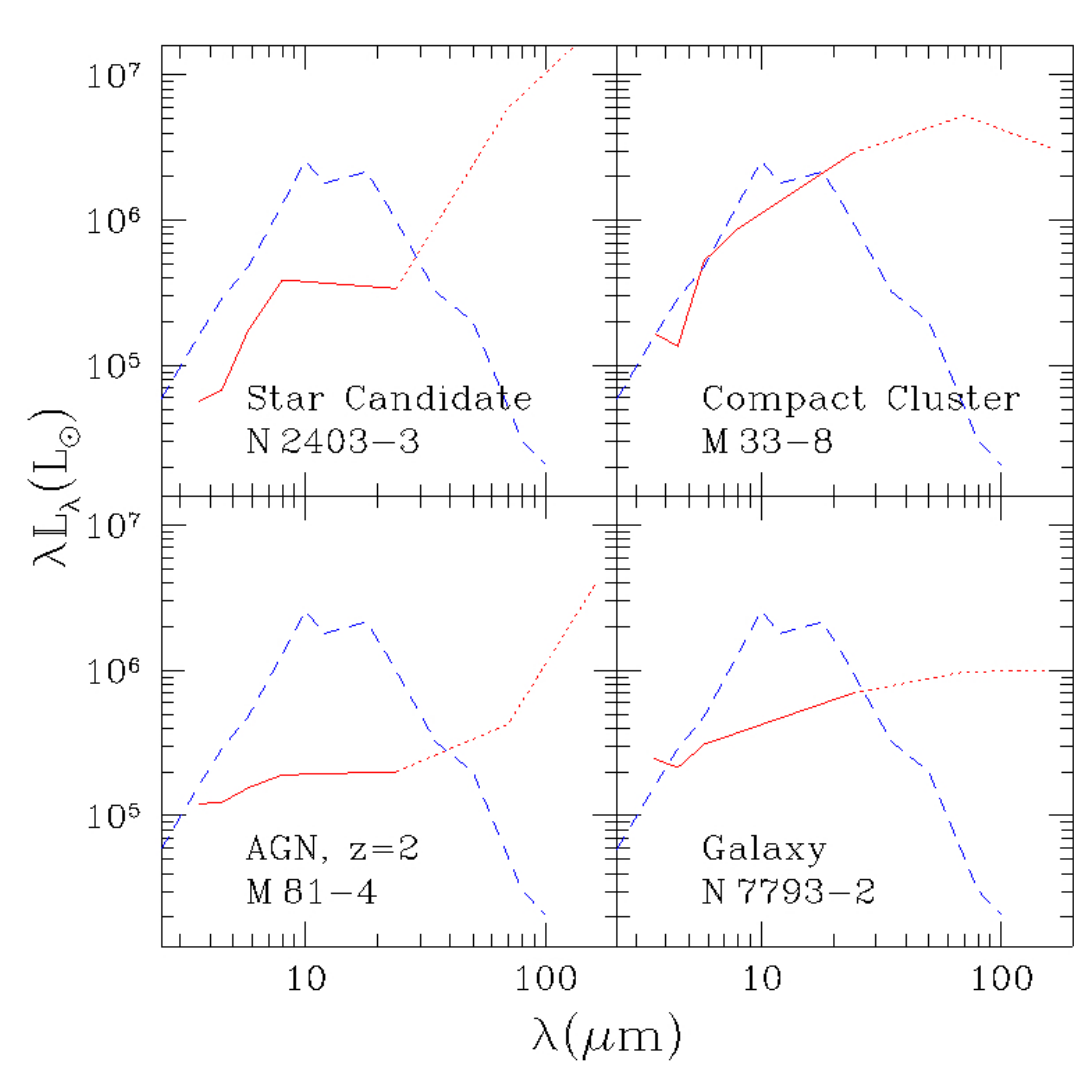


Fig. 4 — (Left) SEDs of four different classes of objects that met our selection criteria: a candidate dusty star in NGC2403, a star-cluster in M33, a QSO behind M81, and a galaxy behind NGC7793. (Right) IRAC and HST images of the compact cluster (top) and the galaxy (bottom). The cluster is a resolved source (FWHM = 0.77" or $\sim 3.6\text{pc}$) in the HST V-band image of the central region of M33 and is very luminous ($2\text{-}3 \times 10^7 L_{\odot}$).

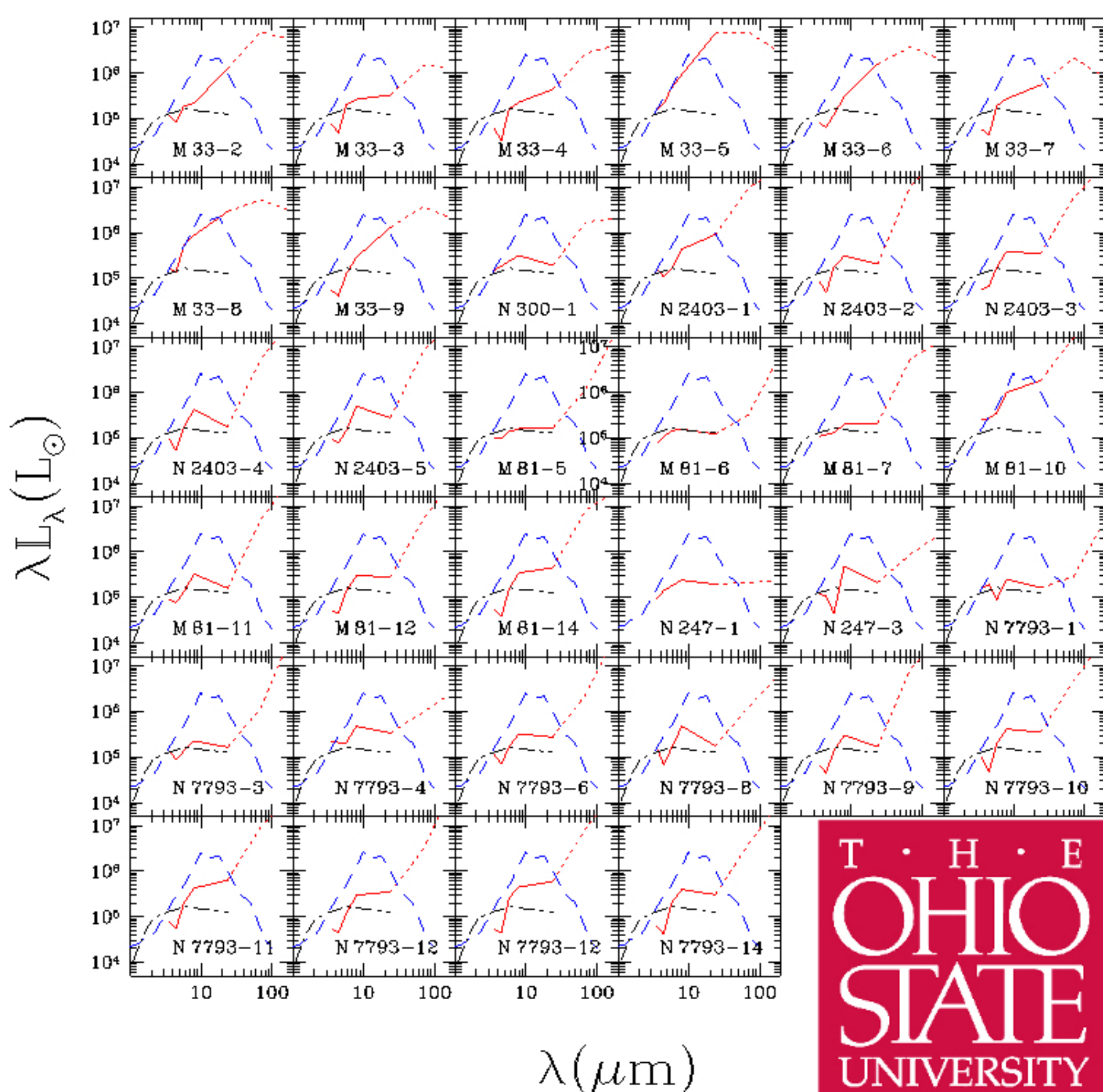
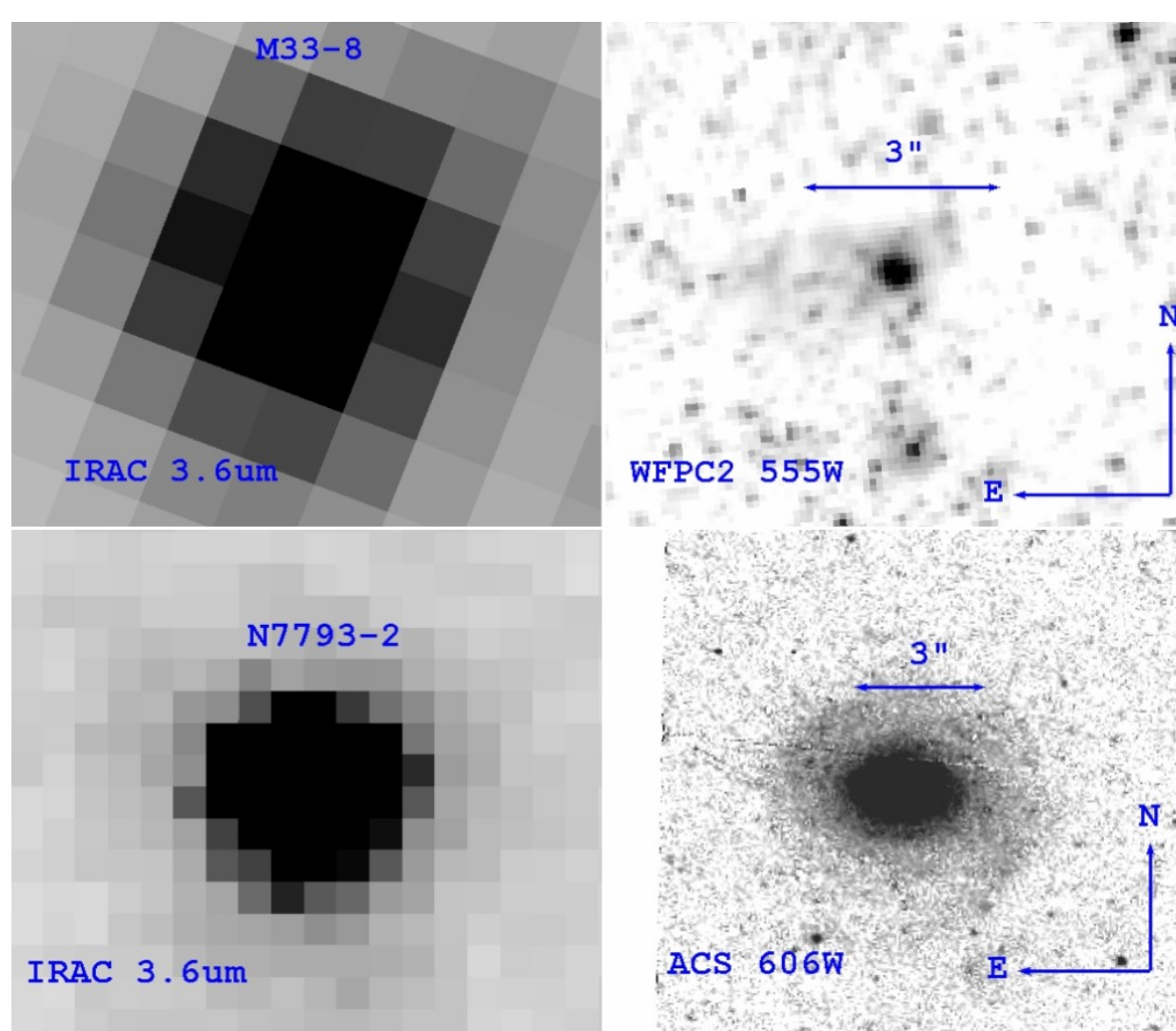


Fig. 5 — SEDs of the 34 sources that met our selection criteria and were *not* rejected due to association with non-stellar sources. The dotted portions of the SEDs correspond to the MIPS 70 and 160 μm flux upper limits. The SEDs of η Car (dashed blue line) and Object X (dot-dashed black line) are shown for comparison. The SEDs of M33-6, M33-10, and M81-10 are similar to η Car while N300-1, M81-5, M81-6 and M81-7 are similar to Object X. On the other hand, the SEDs of some sources, such as N2403-2, N247-3 and N7793-10 are dissimilar and seem unlikely to be stellar sources at all. The MIPS band luminosity limits are useful in less crowded regions. For example, N247-1 is located far away from the disk of the host and probably is a quasar.

This work is supported by NSF Grant AST-1108687



Fig. 2 — The SEDs of η Carinae (Humphreys & Davidson 1994) and "Object X" (Khan et. al. 2011), the brightest mid-IR star in M33. Although the two stars have similar luminosities up to 3.6 μm , the SED of η Car is steeply rising in the IRAC bands (slope ≈ 2.6) while the SED of Object X is almost flat (slope ≈ 0.2).

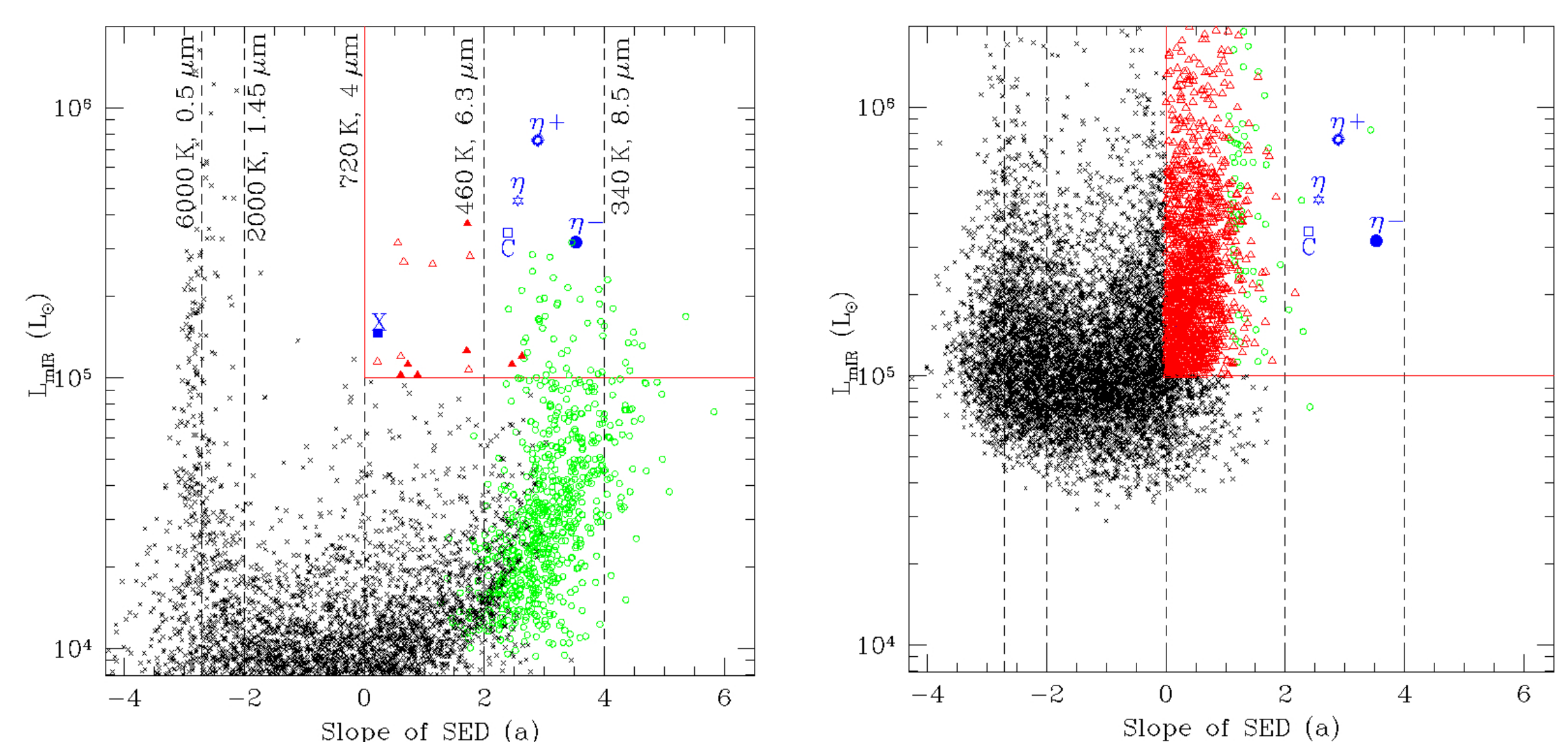
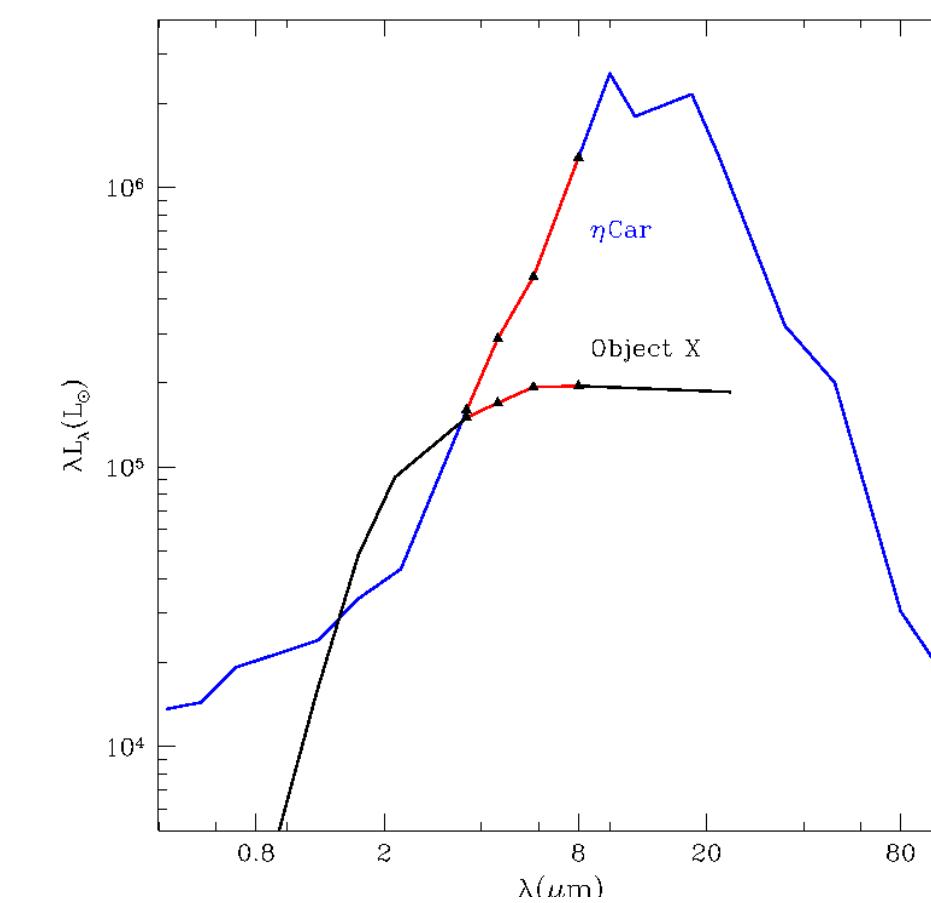


Fig. 3 — (Left) Integrated IRAC band luminosity as a function of the slope a of the mid-IR SED for bright sources in M81. The vertical dashed lines show the slopes of black-bodies with the indicated temperatures and peak wavelengths. The red box shows the candidate selection region. The red triangles show the sources that also satisfy the third selection criteria, that at least 30% of the integrated mid-IR luminosity is emitted between 3.6 and 5.8 μm . Of these, the open red triangles correspond to candidates that are known to be non-stellar in nature and the solid red triangles represent the surviving candidates. The green open circles show sources that do not meet the third selection criteria ($f > 0.3$) and the black cross marks represent all the other sources. The narrow clump of points at slope of ~ -2.75 correspond to normal stars with steeply falling mid-IR SEDs, while the wider clump of points to the right (mostly green circles, sources with $f < 0.3$) correspond to sources dominated by 8 μm PAH emission. The labeled blue points represent objects not in M81 that are shown for comparison: Object X ("X", solid square), the compact cluster M33-8 ("C", open square), η Car ("eta", open star), the η Car cluster excluding η Car itself ("eta-", solid circle; Smith & Brooks 2007), and the η Car cluster including η Car ("eta+", spiked open circle). (Right) The same figure but for sources in a 6 square-degree region of the extragalactic SDWFS Bootes field (Ashby et. al. 2009), transforming their apparent magnitudes to luminosity using M81's distance modulus. 449 ($\sim 75/\text{sq-deg}$) sources pass our selection criteria, indicating that after correcting for area we should expect ~ 13 background sources meeting our selection criteria in the M81 image. Indeed, 7 of the 14 sources in M81 that met our selection criteria were AGNs or galaxies, and are located where we expect to find extragalactic sources.

What Does It Mean?

The core collapse (ccSN) rate in our present sample is of order $R_{\text{SN}} = 0.15/\text{year}$ (3 ccSN in past 20 years). Using simulations with Dusty (Elitzur & Ivezic 2001), we find that eruptions of duration t_e ejecting mass M_e at velocity V_e for a star of luminosity L_{\star} would meet our selection criteria for $t_{\text{detect}} = t_e + 17 (500/V_e \text{ km s}^{-1}) (L_{\star}/10^6 L_{\odot})^{0.75} (M_e/M_{\odot})^{0.073}$ years. The expected number of systems is then $t_{\text{detect}} f_{\eta} R_{\text{SN}}$ if the rate of Great Eruptions is fraction f_{η} of R_{SN} . For systems like η Car where t_{detect} is 50 years or more, we would expect to find roughly $8 f_{\eta} (t_{\text{detect}}/50) (R_{\text{SN}}/0.15)$ systems. Thus in our present, small galaxy sample, we can limit the rate of Great Eruptions to be $f_{\eta} < 0.3$ if none of our candidates survive.

Where Do We Go from Here?

We next need to classify the remaining candidates using HST astrometry and photometry, ground based spectroscopy, and Herschel 70 μm photometry. We can also greatly expand our search to additional galaxies utilizing archival IRAC images from the SINGS, LVL, and S⁴G surveys. More generally, where the poor resolution of *Spitzer* makes the present search challenging, it will be trivial to conduct similar searches at even greater distances using JWST.

References

- Ashby et. al. 2009, ApJ, 701, 428
 Elitzur & Ivezic 2001, MNRAS, 327, 403
 Humphreys & Davidson 1984, Science 223, 243
 Humphreys & Davidson 1994, PASP, 106, 1025
 Khan et. al. 2011, ApJ 732, 43
 Kochanek et. al. 2011, ApJ, 743, 73
 Morse et. al. 1998, AJ, 116, 2443
 Smith & Brooks 2007, MNRAS, 379, 1279